Bletilla striata-derived extracellular vesicles armed probiotic by supramolecular assembly ameliorates colitis via macrophage modulation and microbiota restoration

Weiliang Hou
Second Military Medical University
Kaiwen Sheng
Second Military Medical University
Minxin Gao
Second Military Medical University
Bing Liu
Second Military Medical University
Hao Wang
Second Military Medical University
Xu Li
Second Military Medical University
Yunjie Shi
shiyunpengjie@126.com

Second Military Medical University

Research Article

Keywords: Bletilla striata, supramolecular assembly, probiotic delivery, colitis, macrophage polarization

Posted Date: April 15th, 2026

DOI: https://doi.org/10.21203/rs.3.rs-9332994/v1

Additional Declarations: No competing interests reported.

Version of Record: A version of this preprint was published at Journal of Nanobiotechnology on August 1st, 2026. See the published version at https://doi.org/10.1186/s12951-026-04866-5.

Abstract

Background

Inflammatory bowel disease (IBD) represents major global health challenges, but current treatments often are limited by efficacy loss, infection risks, and disruption of gut homeostasis. Novel therapies are needed to actively promote mucosal repair and restore immune balance.

Results

This study develops a nano-biotherapeutic by conjugating extracellular vesicles derived from *Bletilla striata* (BEVs) with the probiotic *Escherichia coli* Nissle 1917 (EcN) via supramolecular assembly. BEVs contained protocatechualdehyde as a key bioactive metabolite to suppress M1 macrophage polarization and ROS production. EcN@BEVs treatment significantly restored epithelial barrier integrity with the upregulated expression of ZO-1 and Occludin, and reversed microbiota dysbiosis by increasing the Bacillota/Bacteroidota ratio. scRNA-seq and INVADE-seq analyses confirmed that EcN@BEVs promoted a shift from pro-inflammatory to anti-inflammatory macrophage phenotypes and reduced intracellular bacterial invasion.

Conclusions

The EcN@BEVs complex demonstrates significant therapeutic potential for colitis through a multi-faceted mechanism involving enhanced probiotic delivery, direct anti-inflammatory action, gut microbiota restoration, and mucosal immunity reprogramming. This study presents a promising integrated nanotherapeutic strategy for IBD treatment under cross-species collaboration.

1. Introduction

Intestinal inflammation, primarily categorized into inflammatory bowel disease (IBD) and infectious enteritis, represents a major global health burden. IBD, including Crohn's disease (CD) and ulcerative colitis (UC), is a chronic immune-mediated disorder with increasing incidence worldwide, especially in developing regions(1, 2). Infectious enteritis, caused by pathogens such as Salmonella, Campylobacter, and *Clostridioides difficile*, remains highly prevalent and is a leading cause of diarrhea-related morbidity and mortality, particularly in resource-limited settings(3). Current management of IBD relies on immunosuppressants and biologics, which are often limited by primary non-response, secondary loss of efficacy, and significant infection risks(4). For infectious enteritis, antibiotic therapy faces growing challenges due to antimicrobial resistance and disruption of the gut microbiota, which can exacerbate or prolong illness(5). Critically, both therapeutic approaches predominantly focus on suppressing inflammation or eliminating pathogens rather than actively promoting mucosal repair and restoring epithelial barrier function, highlighting a fundamental unmet clinical need(6).

Plant-derived extracellular vesicles (PDEVs) have gained prominence as novel nanotherapeutics for IBD, leveraging their ability to transport bioactive molecules with high biocompatibility and targeted delivery to inflamed tissues(7). Bletilla striata, a traditional medicinal herb, is a particularly promising source of PDEVs due to its well-documented anti-inflammatory and mucosal reparative properties. Key bioactive components, such as polysaccharides (BSP) and stilbenes, have been shown to inhibit pro-inflammatory cytokines and protect against intestinal injury via mechanisms involving the TLR2/MyD88 pathway and oxidative stress attenuation(8, 9). We hypothesize that Bletilla striata-derived EVs (BEVs) may serve as an integrated "drug-carrier" system, naturally encapsulating these therapeutic compounds for enhanced delivery to the gut mucosa, offering a multi-target approach that aligns with the holistic principles of traditional medicine while addressing the limitations of conventional synthetic nanocarriers(10).

The probiotic *Escherichia coli* Nissle 1917 (EcN) exhibits therapeutic efficacy against both IBD and infectious enteritis by immunomodulation, barrier enhancement, and microbiota restoration(11). For infectious enteritis caused by pathogens like Salmonella or *Escherichia coli* O157:H7, EcN acts primarily through competitive exclusion, antimicrobial microcin, and pathogen adhesion disruption (12). However, the therapeutic efficacy of EcN as a single agent is often constrained by its limited gastrointestinal survival, insufficient intestinal colonization, and the complexity of dysbiosis, which frequently results in suboptimal clinical outcomes. These limitations highlight the need for advanced strategies to potentiate probiotic function.

Herein, we engineered a novel nano-biotherapeutic by conjugating BEVs onto the surface of EcN via supramolecular assembly strategy, creating a multifunctional EcN@BEVs system. We systematically evaluated its therapeutic efficacy in both colitis and infectious enteritis models. Our results demonstrate that EcN@BEVs significantly ameliorated intestinal inflammation, restored epithelial barrier integrity, and reversed gut microbiota dysbiosis. Mechanistically, single-cell RNA sequencing and INVADE-seq analyses revealed that EcN@BEVs promoted a shift from pro-inflammatory to anti-inflammatory macrophage phenotypes and reduced intracellular bacterial invasion. This study presents a promising integrated nanotherapeutic strategy for IBD treatment through synergistic modulation of immunity and microbiota (Fig. 1).

The construction of EcN@BEVs via supramolecular assembly and its therapeutic mechanism in colitis through macrophage modulation, microbiota restoration, and epithelial barrier repair.

2. Results

Isolation and Characterization of BEVs

BEVs were isolated from fresh Bletilla striata rhizomes by homogenization in phosphate-buffered saline (PBS) and gradient centrifugation to remove cellular debris and large organelles (Fig. 2A). Transmission electron microscopy (TEM) analysis confirmed that the BEVs exhibited a classical spherical morphology with an intact membrane, consistent with the typical structure of exosome-like nanoparticles (Fig. 2B). Dynamic light scattering (DLS) measurements determined the average hydrodynamic diameter of BEVs

to be 53.14 nm with a surface zeta potential of -6.05 mV (Fig. 2C). Compositional analysis via targeted metabolomics identified protocatechualdehyde as the predominant bioactive metabolite, accompanied by other notable compounds such as dihydromyricetin and luteolin (Fig. 2D), which were widely recognized for their anti-inflammatory and antioxidant activities. Furthermore, polysaccharide composition analysis via ion chromatography revealed that BEV-associated carbohydrates were primarily composed of glucose and mannose at an approximate molar ratio of 2:3 (Fig. S1). The mannose-rich nature of these polysaccharides is notable, as mannose residues can serve as ligands for receptors on immune cells such as macrophages, implying a potential mechanism for targeted immunomodulation. Collectively, these results establish the fundamental physicochemical and compositional profile of BEVs, underscoring their potential as natural nanotherapeutics with intrinsic bioactive properties.

BEVs Modulate M1 Macrophage Polarization and Attenuate Reactive Oxygen Species (ROS) Production

To investigate the immunomodulatory potential of BEVs, we first examined their effect on macrophage polarization using LPS-stimulated RAW264.7 cells. Flow cytometric analysis revealed that BEVs treatment significantly influenced the polarization state in a dose-dependent manner (Figs. 2E, F). Specifically, BEVs reduced the proportion of CD86-positive M1-like macrophages compared to the LPS-only control group. Furthermore, we assessed intracellular ROS levels under the same experimental conditions. BEVs treatment markedly suppressed LPS-induced ROS generation in macrophages, also in a dose-dependent manner (Fig. 2G). To determine whether the observed anti-inflammatory effects were attributable to specific bioactive components within BEVs, we treated LPS-stimulated macrophages with protocatechualdehyde, the predominant metabolite identified in BEVs. Notably, protocatechualdehyde treatment significantly reduced both M1 macrophage polarization and intracellular ROS production (Figs. 2H, I, and S2, 3), suggesting that the anti-inflammatory activity of BEVs is mediated, at least in part, by their key constituent protocatechualdehyde. Overall, these findings demonstrate that BEVs can function as natural nanotherapeutics to suppress pro-inflammatory macrophage activation and oxidative stress, highlighting their potential for mitigating inflammatory responses.

Construction and Characterization of EcN@BEVs

EcN, a well-known probiotic strain widely used for its beneficial effects in modulating host-microbiota homeostasis, synergistically regulating enzyme synthesis, local immunity, and digestion, was selected as the model bacterium (13). To construct an advanced delivery system, we developed a supramolecular assembly strategy to connect EcN with BEVs by pre-modifying the surfaces of two distinct biological membranes with DSPE-PEG-β-CD and DSPE-PEG-ADA (Fig. S4). Upon proximity, these two components undergo a specific "hand-in-hand" recognition via host-guest interaction between β-CD and ADA, facilitating a cytocompatible and facile assembly for targeted delivery (14). Therefore, by employing these two compounds, we connected EcN with BEVs to form an engineered probiotic complex, EcN@BEVs, which is anticipated to possess multi-functional capabilities including gut targeting, anti-inflammatory effects, and microbiota regulation (Fig. 2J).

TEM characterization revealed that spherical BEVs were successfully attached to the outer surface of the bacteria in EcN@BEVs (Fig. 2K). DLS was used to measure the changes in particle size and surface charge after assembly. The results indicated a slight increase in zeta potential (approximately 20 mV) and a significant increase in hydrodynamic size (approximately 150 nm) for EcN@BEVs compared to native EcN (Fig. 2L). The elevation in surface potential is consistent with the inherently higher zeta potential of BEVs, and the increase in particle size corresponds to the attachment of BEVs to the bacterial surface. To further visualize the assembly, BEVs were fluorescently labeled by incubating with FITC (BEVs-FITC), and then connected to EcN, engineered to express mCherry (EcN-mCherry). Subsequent observation by confocal laser scanning microscopy (CLSM) showed clear co-localization of red (EcN-mCherry) and green (BEVs-FITC) fluorescence signals on the assembled complex (Fig. 2M). These results confirm the successful and efficient connection between BEVs and EcN, forming the EcN@BEVs engineered probiotic system.

The cytotoxicity of DSPE-PEG-β-CD, DSPE-PEG-ADA, and BEVs was evaluated using the human colonic adenocarcinoma cell line HT-29. the CCK-8 assay indicated no significant reduction in cell viability after 24 h of co-incubation with DSPE-PEG-β-CD or DSPE-PEG-ADA at concentrations of 25 μM and 50 μM, or with BEVs at concentrations of 50, 100, and 200 μg/ml (Fig. S5). The nanocoating may act as a rigid barrier that obstructs the exchange of matter and energy between the bacteria and their environment, potentially resulting in proliferative suppression of the engineered bacteria. To examine the effect of BEVs conjugation on the growth of EcN, the growth curves of native EcN and EcN@BEVs were monitored by recording the optical density at 600 nm (OD_{600}), showing no significant difference in growth rate (Fig. S6).

Enhanced Gastrointestinal Survival and Mucoadhesion of EcN@BEVs

The ability of orally administered probiotics to survive transit through the upper gastrointestinal tract (GIT) and subsequently achieve prolonged intestinal retention is a critical prerequisite for their therapeutic efficacy (15). Bacterial tolerance to various environmental extremes is crucial for their survival and subsequent colonization in the GIT. Therefore, considering that survival in the low-pH gastric environment is the first major challenge after oral administration, we investigated the survival of native EcN and EcN@BEVs in simulated gastric fluid (SGF). Both unmodified EcN and EcN@BEVs were incubated with SGF supplemented with pepsin. Subsequently, quantitative survival was determined by recording plate counts at predetermined time points. As shown in Fig. 3A, EcN@BEVs exhibited markedly superior tolerance to SGF compared to naked EcN. After 1 h of incubation in SGF, the survival rate of EcN@BEVs was approximately 2-fold higher than that of unmodified EcN. This protective advantage was maintained when the incubation period was extended to 4 h. These observations confirm the potential of BEV conjugation to improve the resistance of probiotics to gastric acid. We speculated that EcN@BEVs might also possess enhanced survival in the intestinal environment. To confirm this, the survival of native EcN and EcN@BEVs upon exposure to bile acids was evaluated. Bile acids have been found to affect the phospholipids and proteins of cell membranes, thereby killing orally administered probiotics (15). After 1 h and 2 h of incubation in bile acids, the survival rate of EcN@BEVs was significantly higher

than that of uncoated EcN (Fig. 3B). In summary, under in vitro conditions, EcN@BEVs demonstrated significantly enhanced survival in both simulated gastric fluid and bile salt solutions, suggesting a superior ability to withstand the upper GIT environment.

After passing through the upper GIT alive, the prolonged retention of probiotics in the intestine is a prerequisite for improving their therapeutic efficacy. To assess intestinal retention in vivo, the distribution and persistence of EcN-GFP and EcN-GFP@BEVs were monitored in mice following oral gavage. The distribution and intestinal retention of EcN were assessed by monitoring fluorescence signals via ex vivo imaging of the gastrointestinal tract using an in vivo imaging system (IVIS) at 4 h and 24 h after oral gavage (Fig. 3C). The fluorescence intensity of unmodified EcN decreased sharply within 24 h after oral administration, indicating that it was only retained in the mouse intestine for approximately 24 h. However, EcN@BEVs could still be detected 24 h post-administration (Figs. 3D, E). These results suggest enhanced survival and retention of the conjugated bacteria in the intestine. To quantify the viable cells in the intestines, the number of live EcN cells within the small intestine, cecum, and colon were separately measured by counting colonies on plates containing kanamycin. Notably, at both 4 h and 24 h post-gavage, the number of EcN@BEVs recovered from the small intestine, cecum, and colon was significantly higher compared to native EcN (Figs. 3F, G, S7). All the above results demonstrate that the survival rate and adhesive capacity of EcN@BEVs in the mouse GIT were significantly improved. These positive results are likely attributable to the effects conferred by conjugation with Bletilla striata BSP-enriched BEVs. The BSP component, known for its excellent film-forming and mucoadhesive properties, can interact with the intestinal mucus layer. This interaction likely forms a protective barrier on the bacterial surface, enhancing resistance to gastric acid and bile salts, while simultaneously promoting prolonged intestinal residence through improved adhesion to the mucosal epithelium.

Therapeutic Efficacy of EcN@BEVs in DSS-Induced Mouse Colitis Model

Encouraged by the anti-inflammatory properties of Bletilla striata-derived nanoparticles and the high survival rate and potent intestinal adhesion capabilities of encapsulated probiotics, we evaluated their potential as an oral therapeutic agent for acute colitis in a mouse model of DSS-induced acute colitis.

After 6 days of exposure to 3% DSS to induce acute colitis, mice were orally administered 5×10^8 CFU EcN@BEVs daily for 5 days (Fig. 4A). Uncoated EcN, Bletilla striata-derived nanoparticles and phosphate-buffered saline (PBS) were used as the controls. Mice treated with EcN@BEVs exhibited a rapid improvement in body weight, whereas other treatments failed to effectively prevent weight loss (Fig. 4B). Colitis typically induces detrimental inflammatory responses, resulting in a reduction of colon length and splenomegaly. Therefore, the colon length and the splenic index of each mouse were measured post-treatment. Mice treated with EcN@BEVs exhibited the longest average colon length and the lowest splenic index, which most closely approximated those of the healthy control. Importantly, the average colon length and splenic index in the EcN@BEVs group were more favorable than those in the other group, indicating that the EcN@BEVs treatment confers superior therapeutic efficacy relative to the uncoated EcN and Bletilla striata-derived nanoparticles (Figs. 4C-F).

Hematoxylin and eosin (H&E) staining of colon tissues revealed varying degrees of histological improvement across all treatment groups compared to the DSS + PBS group. The DSS + PBS group exhibited severe inflammatory damage, characterized by complete crypt loss, goblet cell depletion, and extensive immune cell infiltration. In contrast, the EcN@BEVs group showed remarkable restoration, featuring intact epithelial structure and minimal inflammatory cell infiltration (Fig. 4G). Furthermore, H&E staining of splenic tissues indicated that DSS treatment significantly increased inflammatory cell infiltration in the spleen, which was substantially attenuated by EcN@BEVs administration (Fig. 4G). Furthermore, EcN@BEVs not only significantly mitigated DSS-induced impairment of intestinal barrier integrity, as evidenced by the upregulated expression of tight junction proteins including ZO-1 and Occludin (Figs. 4H-J), but also markedly alleviated DSS-triggered immune activation, with immunohistochemical staining revealing a significant reduction in the number of IL-6, TNF-α, and MPO-positive cells following EcN@BEVs administration (Fig. S8).

These results demonstrate that EcN@BEVs possesses excellent therapeutic efficacy in the mouse model of DSS-induced acute colitis. This efficacy is mainly dependent on the anti-inflammatory properties of Bletilla striata-derived nanoparticles and the enhanced survival and mucosal adhesion of EcN@BEVs in the intestine.

Regulation of the Gut Microbiota by EcN@BEVs in Colitic Mice

Dysbiosis of the gut microbiota was one of the main causes of colitis, including the decrease in microbial diversity and the changes in microbial composition. Therefore, the mouse feces were collected and subjected to 16S rRNA sequencing to study the impact of EcN@BEVs on the gut microbiota of colitic mice. The α diversity indices, such as the Chao1 index and Shannon index, can indicate the richness and diversity of bacterial composition. Compared with the DSS group, the α diversity of the gut microbiota was increased with the treatment of EcN@BEVs, indicating that EcN@BEVs could improve microbial ecological dysbiosis (Fig. S9). The differences in the microbial β diversity among samples were assessed using principal coordinate analysis (PCoA) and the unweighted pair-group method with arithmetic means (UPGMA) (Figs. 5A, B). A Bray-Curtis distance metric was employed for the PCoA. The results revealed that mice treated with EcN@BEVs formed a distinct cluster separate from that of the DSS-induced colitis mice, while such separation was not observed among the other two groups (the DSS + EcN group, and the DSS + BEVs group) (Fig. 5A). Furthermore, healthy mice and EcN@BEVs-treated colitic mice clustered more closely together compared to mice from the remaining groups. UPGMA hierarchical clustering analysis demonstrated high similarity among biological replicates within each experimental group. The EcN@BEVs treatment group showed low similarity to the DSS-induced colitis group but clustered more closely with the healthy control group (Fig. 5B), indicating that EcN@BEVs could positively restore the gut microbiota composition in colitic mice and was more effective than other probiotic treatments.

Subsequent analysis at the phylum level focused on the differential bacterial taxa between the DSS-induced colitis group and the EcN@BEVs-treated group. Bacillota (formerly Firmicutes) and Bacteroidota

collectively accounted for over 90% of the total bacterial community. Compared to the DSS group, the EcN@BEVs treatment group showed a significant decrease in the relative abundance of Bacteroidota and an increase in the relative abundance of Bacillota (Fig. 5C). Furthermore, statistical analysis of the Bacillota/Bacteroidota ratio across groups revealed a significant elevation in the EcN@BEVs-treated group (Fig. 5D). The Bacillota/Bacteroidota ratio is widely acknowledged as a crucial factor in maintaining gut homeostasis, and its decrease is commonly associated with inflammatory bowel disease (IBD) (16). Further analysis of the microbial composition at family level indicated that the EcN@BEVs treatment significantly increased the abundance of Lachnospiraceae (Figs. 5E, F). Heatmap analysis was then used to investigate the composition of gut microbiota at the genus level. Compared with the DSS group, EcN@BEVs treatment effectively increase the abundance of *Helicobacter* and *Lachnospiraceae_NK4A136_group* (Figs. 5G-I). Linear discriminant analysis Effect Size (LEfSe) was used to identify the characteristic bacteria among PBS, DSS and EcN@BEVs treatment groups. Consistent with the aforementioned findings, the main characteristic bacteria in the DSS group was Bacteroidales. In contrast, the probiotic Lachnospirales was identified as the characteristic bacteria in the EcN@BEVs treatment group (Fig. 5J). These results suggest that EcN@BEVs treatment can restore gut microbiota in the experimental colitis model, which can potentially suppress inflammation and promote the healing of lesions.

Therapeutic Efficacy of EcN@BEVs in Salmonella-Induced Mouse Colitis Model

To further evaluate the therapeutic effect of EcN@BEVs on acute enteritis, we employed an attenuated Salmonella typhimurium strain, VNP20009, engineered to express mCherry (VNP20009-mCherry), to induce acute colitis in mice for subsequent investigation. Mice were first pretreated with streptomycin sulfate via oral gavage to deplete the resident gut microbiota, followed by infection with VNP20009-mCherry (2×10^7 CFU per mouse) to establish acute colitis. Treatment with EcN, BEVs, or EcN@BEVs was administered every other day post-infection, with sacrifice and sample collection performed on day 6 (Fig. 6A). Salmonella infection induced severe manifestations, resulting in 100% mortality within 8 days in the untreated group and a significant reduction in colon length. However, treatment with EcN@BEVs completely reversed these outcomes, while only one death occurred in the EcN@BEVs-treated group within the same period (Fig. 6B), and colon length was restored to a level comparable to that of healthy controls (Figs. 6C, D). On day 6 post-infection, the bacterial load of VNP20009 in the colons of untreated mice reached a high level of approximately 5×10^7 CFU/mg. Compared to the untreated group, administration of EcN@BEVs significantly reduced the Salmonella burden, although it did not achieve complete eradication (Figs. 6E, F, and S10). Consistent results were observed in frozen intestinal sections by detecting the intrinsic red fluorescence of VNP20009-mCherry (Fig. S11). Histopathological analysis via H&E staining indicated that EcN@BEVs treatment effectively attenuated the severe pathological damage in the colonic tissues of infected mice (Fig. 6G). Immunofluorescence staining further revealed that Salmonella infection markedly increased the expression of IL-1β and the number of $F4/80^+IL\text{-}1\beta^+$ pro-inflammatory macrophages in the colonic mucosa. In contrast, EcN@BEVs treatment reduced IL-1β expression and significantly decreased the abundance of $F4/80^+IL\text{-}1\beta^+$ macrophages,

suggesting a potential role in inhibiting pro-inflammatory macrophage polarization (Fig. 6H-J). Collectively, these results demonstrate that EcN@BEVs treatment alleviates intestinal damage caused by Salmonella infection, likely attributable to its combined bactericidal and anti-inflammatory properties.

EcN@BEVs Attenuates Colitis through the Regulation of Macrophages

To gain a comprehensive understanding of the immunoregulatory mechanisms by which EcN@BEVs ameliorate Salmonella-induced colitis, we performed single-cell RNA sequencing (scRNA-seq) on colonic cells isolated from mice on day 6 post-infection, comparing untreated colitic mice with those treated with EcN@BEVs. A total of 13,439 high-quality cells were assigned to 13 distinct cell clusters using unbiased graph-based clustering (UMAP) (Fig. S12A). Treatment with EcN@BEVs significantly altered the global cellular composition, as evidenced by changes in the proportions of various clusters (Figs. S12B, C). Notably, the treatment increased the proportions of T cells and B cells, suggesting that EcN@BEVs can enhance Salmonella-specific adaptive immunity, potentially through cytotoxic T-cell activity and antibody production, even at a late infection stage. Concurrently, the proportion of macrophages decreased, indicating a potential suppression of excessive innate immune activation. We subsequently focused on the macrophage population (totally 1,489 cells), identified by canonical marker genes (CD68, C1qa, Apoe) (Figs. 7A, S13A). Sub-clustering of these cells yielded three distinct macrophage subpopulations (Clusters 1–3). EcN@BEVs treatment markedly reduced the proportion of Cluster 1 while significantly increasing the proportions of Clusters 2 and 3 (Figs. 7B, C). Differential gene expression analysis revealed that Cluster 1 exhibited a strong pro-inflammatory signature, characterized by high expression of genes such as Nlrp3, Il1b, CD86, and Cxcl2 (Figs. 7D-F). In contrast, Cluster 2 predominantly expressed anti-inflammatory genes including Apoe and C1qa, while Cluster 3 was enriched in genes associated with tissue repair and chemotaxis, such as Mrc1, Folr2, and Cd163 (Fig. 7D). Scoring based on inflammatory gene modules confirmed Cluster 1 as pro-inflammatory macrophages, and Clusters 2 & 3 as anti-inflammatory macrophages (Figs. 7G, H). Thus, EcN@BEVs treatment effectively reduced pro-inflammatory macrophages while promoting an anti-inflammatory macrophage phenotype. This shift was corroborated by immunofluorescence staining of colon tissues, which showed that Salmonella infection significantly increased $F4/80^{+}IL\text{-}1\beta^{+}$ cells, an effect that was reversed by EcN@BEVs treatment (Figs. 6J, K).

GO enrichment analysis of differentially expressed genes in colonic epithelial cells (Fig. S13B) further demonstrated significant downregulation of the response to bacterium and the immune system process signaling pathways indicating that EcN@BEVs treatment substantially suppressed inflammatory responses and reduced reactivity to bacterial infection in the epithelial compartment (Fig. 7I).

Furthermore, Invasion-adhesion-directed expression sequencing (INVADE-seq) was employed to profile intracellular bacteria within host cells. We found that the number of bacteria detected in mouse intestinal cells significantly increased after Salmonella infection, which may be related to Salmonella disrupting the intestinal barrier. Following treatment with EcN@BEVs, the number of detected bacteria decreased, suggesting that intestinal barrier function may have been restored (Fig. 7J). In the

Salmonella-infected group, the primary bacteria detected in mouse colons included Escherichia, Shigella, Helicobacter, and other pathogens capable of damaging colonic cells. Additionally, a small amount of Salmonella was detected. In contrast, the EcN@BEVs-treated group showed a significant reduction in Escherichia and Shigella, with no Salmonella detected within cells (Fig. 7K).

These results collectively indicate that EcN@BEVs provide protection against Salmonella-induced colitis through a coordinated mechanism involving the enhancement of adaptive immunity (T and B cells) to combat the pathogen, thereby reducing its invasive effects on the colonic epithelium. Concurrently, by suppressing pro-inflammatory macrophages and activating anti-inflammatory macrophages, it inhibits inflammatory responses in colonic tissue and promotes the restoration of the colonic epithelial barrier function.

3. Discussion

IBD represent significant clinical challenges due to their rising incidence and profound impact on patient quality of life. These disorders are characterized by chronic inflammation of the gastrointestinal tract, leading to compromised mucosal integrity and dysregulated immune responses. Conventional therapeutic options often face limitations including loss of efficacy, adverse effects. Moreover, infectious enteritis treatment is complicated by the emergence of antibiotic resistance and gut microbiota dysbiosis, underscoring the urgent need of innovative interventions by restoring epithelial barrier function and promoting mucosal healing(17, 18). Notably, while nanocarriers hold great promise for targeted drug delivery, their potential to induce unintended inflammatory responses through mechanisms such as mitochondrial dysfunction, lysosomal damage, and inflammasome activation has raised significant safety concerns(19). Therefore, the use of naturally-derived vesicles, which exhibit intrinsic bioactivity and low immunogenicity, may offer a safer alternative for engineering probiotic-based therapeutic systems. In this study, our study explores a novel therapeutic strategy by integrating PDEVs isolated from Bletilla striata on the surface of probiotic EcN to efficiently achieve intestinal inflammation attenuation, gut microbiota restoration, and epithelial barrier repair.

The enhanced adherence and viability of EcN@BEVs under simulated gastrointestinal conditions underscore their potential to overcome the hostile gut environment. The approximately twofold increase in survival rates following exposure to gastric acid and bile salts suggests that the BEVs confer protective effects for EcN(20). Improved adhesion may be attributable to surface molecules on BEVs that promote mucosal interactions, facilitating colonization and sustained probiotic activity. This contrasts with conventional probiotic formulations that frequently exhibit limited survival and transient colonization, thereby reducing therapeutic impact. Notably, recent advances in microbiota transplantation strategies, such as single-cell nanocapsulation of gut microbes, have similarly aimed to enhance bacterial viability and targeted delivery, supporting the translational potential of nano-engineered probiotic systems(21). These findings demonstrated the nanovesicle-mediated enhancement of bacterial resilience and mucosal attachment, presenting a methodological advancement for live bacteria administration.

EcN@BEVs manifest superior therapeutic outcomes in DSS-induced colitis models by immune modulation, enhanced bacterial survival, and microbiota restoration. Importantly, the nanoparticle-like properties of BEVs facilitate targeted delivery of bioactive compounds and probiotics to inflamed tissues, overcoming limitations of systemic drug distribution and degradation(20, 22). Notably, protocatechualdehyde, the predominant bioactive metabolite identified in BEVs, was found to directly suppress M1 macrophage polarization and reduce ROS production in a dose-dependent manner in vitro, suggesting that BEVs contribute not only as a delivery vehicle but also as an active therapeutic component. This bioactive molecule likely acts by interfering with NF-κB signaling or other inflammatory pathways, thereby amplifying the anti-inflammatory effects of the probiotic cargo. Thus, the intrinsic pharmacological activity of BEVs synergizes with EcN-mediated immunomodulation, creating a dual-action therapeutic platform that simultaneously delivers both a drug and a drug carrier. This integrated pharmacological approach highlights an innovative modality combining biological and nanotechnological tactics to enhance efficacy in intestinal inflammation treatment.

The immunomodulatory effects of EcN@BEVs are evidenced by their capacity to skew macrophage polarization from a pro-inflammatory M1 phenotype toward an anti-inflammatory M2 phenotype. This shift is accompanied by upregulated expression of anti-inflammatory genes such as Apoe and C1qa and downregulation of pro-inflammatory mediators, indicating suppression of innate immune overactivation. These findings align with prior reports identifying macrophage plasticity as a pivotal determinant in intestinal inflammation resolution and repair(23). The modulation of inflammasome components further suggests that EcN@BEVs may attenuate caspase-1 activation and subsequent IL-1β maturation. Notably, the single-cell RNA sequencing approach reveals cell-type-specific transcriptional changes, surpassing bulk analyses in resolving immune heterogeneity. Unlike traditional immunosuppressive therapies, EcN@BEVs recalibrate macrophage functional states, potentially preserving host defense by reducing tissue damage. This immunoregulatory mechanism thus represents a targeted intervention at the level of macrophage polarization, distinct from systemic cytokine blockade strategies. Moreover, the ability of EcN@BEVs to restore gut microbiota composition and diversity echoes findings from whole microbiota transplantation studies (24). This parallel underscores the importance of microbiota modulation in managing inflammatory and infectious intestinal disorders. In parallel with therapeutic innovations, recent advances in non-invasive diagnostic biomarkers—such as the circulating cfDNA miR-129-2 promoter methylation marker for early detection of advanced adenoma and colorectal cancer—underscore the importance of integrating early diagnosis with targeted intervention to optimize patient outcomes(25).

4. Conclusions

In summary, this study highlights the significant role of EcN@BEVs in modulating gut immunity, enhancing cellular viability, and restoring microbial balance, alongside their promising pharmacological effects. The exploration of underlying mechanisms and potential applications suggests that EcN@BEVs could emerge as an innovative therapeutic strategy for treating colitis and related disorders. Future research should focus on larger, multicenter clinical trials to validate these findings and investigate the

long-term implications of EcN@BEVs in clinical settings, thereby enriching the landscape of IBD treatment options.

5. Materials and Methods

Chemicals and Reagents

Phosphate-buffered saline (PBS) was obtained from Servicebio. Lipopolysaccharide (LPS, L2880) was purchased from Sigma Aldrich. CD86-APC and F4/80-PE were supplied by Biolegend. Dextran sulfate sodium salt (DSS, MW: 36–50 kDa) was obtained from MP Biochemicals. Reactive Oxygen Species (ROS) Fluorometric Assay Kit (Green) was acquired from Elabscience. Protocatechualdehyde was purchased from MedChemExpress. DSPE-PEG-β-CD and DSPE-PEG-ADA were obtained from Xian Ruixi Biological Technology Co., Ltd. FITC was purchased from MedChemExpress. Luria-Bertani (LB) medium, kanamycin, streptomycin sulfate, and agar were purchased from Biosharp. Bile salts and pepsin powder were obtained from Solarbio. Anti-ZO-1 antibody was purchased from Affinity. Anti-Occludin antibody was purchased from Beyotime Biotechnology. Anti-IL-6 antibody was obtained from Servicebio. Anti-MPO antibody and anti-TNFα were purchased from Abcam. Anti-IL-1β antibody and anti-F4/80 antibody were obtained from Cell Signaling Technology. Goat anti-Rabbit IgG (H + L) Cross-Adsorbed Secondary Antibody, Alexa Fluor™ 488 was purchased from Invitrogen.

Bacterial Strains and Animals

EcN was purchased from the China General Microbiological Culture Collection Center and cultured in Luria-Bertani (LB) medium at 37°C with 50μg/ml kanamycin. *Salmonella typhimurium* VNP20009 was obtained from Shanghai Microbiological Culture Collection Center and cultured in Luria-Bertani (LB) medium at 37°C with 50μg/ml kanamycin.

Male BALB/c mice aged 6–8 weeks were obtained from Hangzhou Ziyuan Laboratory Animal Technology Co., Ltd. All mice were raised in specific pathogen-free (SPF) conditions in the Laboratory Animal Center of the Naval Medical University (Shanghai, China). The experiments were approved by the Laboratory Animal Center of the Naval Medical University in conformance with the National Institute of Health Guide for the Care and Use of Laboratory Animals.

Cell Culture and LPS-Induced Inflammation Model

The RAW264.7 cells were procured from QuiCell. The RAW264.7 cells were cultured in DMEM (Gibco) containing 10% FBS at 37°C with 5% CO2. Cells were subcultured at 80–90% confluence by gentle scraping, followed by reseeding at an appropriate dilution into fresh culture flasks. The RAW264.7 cells were modelled using 1 μg/mL LPS for 24 h.

Preparation of Bletilla striata Extracellular Vesicles (BEVs)

Bletilla striata rhizomes were washed, peeled, cut into small pieces, and placed into cold phosphate buffer saline (PBS, pH = 7.2) with a weight/volume ratio of 1:4, and homogenized in a blender. The BEVs were obtained via gradient centrifugation following 1000 g for 20 min, 5000 g for 40 min, and 10,000 g for 1 h. The resultant BEVs were stored at -80℃.

Targeted Flavonoid Metabolomics Analysis

The targeted flavonoid metabolomics analysis was undertaken by Gideon Biotechnology Co., Ltd. (Guangzhou, China). Sample extracts were prepared using methanol/water/formic acid (15:4:1, v/v/v) with 0.5% BHT, purified by solid-phase extraction, and analyzed by LC-MS/MS. Chromatographic separation was performed on a Waters UPLC system (BEH C18/HSS T3 column) with a methanol/10 mM ammonium formate gradient. Detection and quantification were achieved using an AB Sciex 5500 QQQ-MS in MRM mode with external calibration standards. Quality control samples were analyzed to ensure system stability.

In Vitro Assessment of Anti-Inflammatory Properties

RAW 264.7 macrophage cells were cultured in 24-well plates at 37°C for 24 h and washed with PBS. Subsequently, BEVs and protocatechualdehyde were cultured with RAW 264.7 cells in the absence or presence of lipopolysaccharide (LPS) (1 μg/mL) for 24 h. The cultured RAW264.7 cells were labelled with the ROS probe (10 μM DCFH-DA) for flow analysis (CytoFLEX, Beckman, USA), or stained with APC-conjugated anti-CD86 antibody and PE-conjugated anti-F4/80 antibody to detect M1 macrophage polarization by flow analysis (CytoFLEX, Beckman, USA).

Preparation of EcN@BEVs

EcN was cultured in 5 mL of LB medium at 37°C for 16h. And then EcN cells (1×10^9 CFU) were washed with PBS, followed by resuspension in 500 μL PBS solution. Thereafter, the DSPE-PEG-β-CD and DSPE-PEG-ADA were dissolved in DMSO and diluted to 1 mM with PBS. 25 μL of DSPE-PEG-β-CD (1 mM) solution was added to 500 μL of EcN solution, and the mixture was incubated at 37°C and 150 rpm for 1 h. 25 μL of DSPE-PEG-ADA (1 mM) solution was added to 500 μL of BEVs solution, and the mixture was incubated at 37°C and 150 rpm for 1 h. Afterward, the two mixtures were combined and incubated at 37°C with constant rotation for 30 minutes, resulting in the formation of EcN@BEVs. EcN@BEVs were then washed with PBS twice.

Characterization of BEVs and Coated Probiotics

The apparent zeta potential and size distribution of native BEVs, EcN, and EcN@BEVs were measured by a Zetasizer Nano ZS instrument (Malvern, UK). The morphology of BEVs, EcN, and EcN@BEVs was visualized by Transmission Electron Microscope (TEM, Hitachi HT7800, Japan). For each assay, a drop of solution was deposited onto a glow-discharged, carbon-coated copper grid for 1 minute. 10 μl of uranyl acetate solution was applied onto the copper grid and allowed to settle for 1 minute. The sample was air-dried at room temperature for several minutes, and then imaged using electron microscopy at 80

kV. To intuitively visualize the EcN@BEVs, the BEVs were labeled with FITC via a post-functionalized process. The EcN@BEVs were characterized by the confocal laser scanning microscope (CLSM, ZEISS LSM980, Germany).

Measurement of Growth Curves

The EcN and EcN@BEVs were diluted in 10 mL of fresh LB medium and incubated at 37°C with gentle shaking. The OD_{600} value was measured in triplicate for 12 h at 2 h intervals by a microplate reader (Synergy H4, BioTek, USA).

Resistance Assay in Vitro

An equal amount of native EcN and EcN@BEVs was separately resuspended into 1 mL simulated gastric fluid (SGF, pH = 2.0, each 20 mL of ddH_2O containing 0.2g pepsin, pH was adjusted to 2.0 with HCl) or bile acid (0.3mg/mL) and further incubated at 37°C with gentle shaking. At predetermined time points, 100 μL of each sample was taken, washed with PBS, and spread on the LB agar plate with an appropriate dilution. The colonies were counted after incubation at 37°C for 24h.

Adhesion Observation in Vivo

To evaluate the survival rate and adhesive capacity of coating probiotics in vivo, EcN-GFP, was encapsulated and orally administered to mice. The native EcN-GFP was used as a control. The distribution of coated probiotics in the GIT was monitored through fluorescent signals via IVIS (VISQUE® Invivo Smart-LF, Vieworks, Korea). Briefly, BALB/c mice were randomly and equally divided into two groups (n = 3 in each group) and administered an equal amount (1×10^8 CFU) of EcN-GFP and EcN-GFP@BEVs. The intestines were harvested at 4 h and 24 h post administration and visualized under an IVIS. In addition, intestinal tract tissues, including the small intestine, colon, and cecum, as well as their inside contents, were collected and homogenized in 1 mL PBS, followed by diluting and spreading onto solid LB agar plates at 37°C for counting.

DSS-induced Colitis Model

BALB/c mice (male, 6–8 weeks) were fed 3% DSS salt in sterile drinking water for 6 days. Mice were randomly divided into five groups (n = 5) and administered PBS, EcN (1×10^8 CFU/mouse/day), BEVs (100 μL), or EcN@BEVs (1×10^8 CFU/mouse/day) via oral gavage for 4 days. On day 11, mice were sacrificed. The colons and spleens of mice were collected for length and weight measurement, as well as histopathological analysis.

Salmonella typhimurium-induced Colitis Model

BALB/c mice (male, 6–8 weeks) were treated with 100 μl streptomycin solution (200 mg/mL) before infection by oral inoculation with 2×10^7 CFU of VNP20009. Mice were randomly divided into five groups (n = 6) and treated with PBS, EcN (1×10^8 CFU/mouse/day), BEVs (100 μL), or EcN@BEVs (1×10^8

CFU/mouse/day) on days 2 and 4 post-infection. Mice were weighed daily and sacrificed on day 6 post-infection. The colons of mice were collected for length measurement and histopathological analysis.

Histological and Immunohistochemical Analysis

Colon and spleen tissues were fixed in 4% neutral buffered formalin, embedded in paraffin, and sectioned at 4 μm thickness. For histological evaluation, sections were stained with H&E. Immunofluorescence (IF) and immunohistochemistry (IHC) staining were performed according to the manufacturers' protocols using respective primary and secondary antibodies. All tissue images were captured using a 3D HISTECH Pannoramic 250 (3DHISTECH, Hungary).

16S rRNA Analysis of Fecal Samples

The 16S rRNA analysis was undertaken by Gideon Biotechnology Co., Ltd. (Guangzhou, China). The total genomic DNA was extracted according to the instructions of the HiPure Stool DNA Kit, and the DNA was quantified and its quality was evaluated by NanoDrop and agarose gel, respectively. The extracted DNA was diluted to a concentration of 1 ng/μL and stored at -20°C until further use. The 16S rRNA gene of bacteria was amplified by PCR using diluted DNA as a template with barcode primers and Takara Ex Taq (Takara, Tokyo, Japan). Universal primers 341 F and 806 R were used to amplify the V3-V4 variable region of the 16S rRNA gene. The primers were linked to Illumina sequencing adapters, and the reverse primer contained the sample barcode. The PCR products were purified, adjusted for concentration, and sequenced on an Illumina Novaseq 6000 system. Clean tags were clustered into OTUs at ≥ 97% similarity using the UPARSE algorithm in USEARCH (version 9.2.64). Chimeras in tags were checked using the UCHIME algorithm. Effective tags obtained after filtering chimeras were used for OTU abundance statistics and subsequent analyses. The most abundant tag sequence within each OTU was selected as its representative sequence.

Single-cell transcriptome and INVADE-Seq library preparation

Single-cell transcriptome and INVADE-Seq library preparation were undertaken by Oebiotech Corporation (Shanghai, China). Chromium Next GEM Single Cell 5' Kit v2 (10x Genomics, PN-1000263) was used for scRNA-seq and INVADEseq according to the User Guide (CG000331). Single cell suspension was adjusted to 700–1200 cells/μL. Cells were mixed with reverse transcription Master Mix, 16S primer (5'-GGGTTGCGCTCGTTG-3', final concentration 16 μmol/L), and loaded into a Chromium chip K with gel beads and partitioning oil to generate GEMs on a 10x Chromium Controller, followed by reverse transcription PCR and preamplification of the full-length cDNA. The cDNA QC was performed using Agilent 4150 TapeStation (Agilent Technologies). The cDNA was used to construct the transcriptome sequencing library using a 10x Genomics Library Construction Kit (PN-1000190). High-throughput sequencing was performed on the Illumina NovaSeq X Plus sequencer with PE-150 mode. For INVADE-Seq, 16S rRNA enrichment was performed with custom primers (FP: 5'-GATCTACACTCTTCCCTACACGACGCTCTTCCGATCT-3'; RP:5'-

GTGACTGGAGTTTCAGACGTGTGCTCTTCGCATCTTCACGRCACGAGCTGACGAC-3') in a two-round PCR amplification (35 and 20 cycles, respectively), followed by size selection (955–1,215 bp) and dual-indexing using the Chromium Dual Index Kit TT Set A (PN-1000215). All libraries were sequenced on an Illumina NovaSeq X Plus platform with PE-150 mode.

Statistical Analysis

Statistical analysis was performed with GraphPad Prism (GraphPad Software Inc, La Jolla, CA, USA). Compared samples between groups using ANOVA. Differences in survival of the various mouse groups were compared using the Kaplan-Meier analysis and Cox regression analysis. The GraphPad software generated a P value and statistic for each analysis; $P < 0.05$ was considered statistically significant. Combining the species/OTU relative abundance and the transcriptome gene expression data, correlations between the species/OTUs and the genes were evaluated using Pearson's correlation algorithms.

Declarations

Ethics approval statement: This study was approved by the Ethics Committee of the Naval Medical University(Reference: NMUMREC-2021-005, Research Proposal No.: 20210310005, Conference Date: March 10, 2021) per the Declaration of Helsinki.

Data availability statement: The data that support the findings of this study are available from the corresponding author upon reasonable request.

Funding statement: This work was supported by the 78th of China Postdoctoral Science Foundation (NO. 2025M784489).

Conflict of interest disclosure: The authors declare no conflict of interest in this work.

Author contributions

Weiliang Hou: conceived and designed the project. Kaiwen Sheng: conducted basic research experiments. Minxin Gao: collected the data. Bing Liu: collected the data. Hao

Wang: conceived and designed the project. Xu Li: conceived and designed the project. Yunjie Shi: conceived and designed the project. All authors have read and approved the final manuscript.

Acknowledgements

None.

References

1. Ng SC, Shi HY, Hamidi N, Underwood FE, Tang W, Benchimol EI, et al. Worldwide incidence and prevalence of inflammatory bowel disease in the 21st century: a systematic review of population-based studies. Lancet. 2017;390(10114):2769–78.
2. Kaplan GG, Windsor JW. The four epidemiological stages in the global evolution of inflammatory bowel disease. Nat Rev Gastroenterol Hepatol. 2021;18(1):56–66.
3. Estimates of the. global, regional, and national morbidity, mortality, and aetiologies of diarrhoea in 195 countries: a systematic analysis for the Global Burden of Disease Study 2016. Lancet Infect Dis. 2018;18(11):1211–28.
4. Roda G, Jharap B, Neeraj N, Colombel JF. Loss of Response to Anti-TNFs: Definition, Epidemiology, and Management. Clin Transl Gastroenterol. 2016;7(1):e135.
5. Langdon A, Crook N, Dantas G. The effects of antibiotics on the microbiome throughout development and alternative approaches for therapeutic modulation. Genome Med. 2016;8(1):39.
6. Chang JT. Pathophysiology of Inflammatory Bowel Diseases. N Engl J Med. 2020;383(27):2652–64.
7. Teng Y, Ren Y, Sayed M, Hu X, Lei C, Kumar A, et al. Plant-Derived Exosomal MicroRNAs Shape the Gut Microbiota. Cell Host Microbe. 2018;24(5):637–e528.
8. Jiang S, Wang M, Jiang L, Xie Q, Yuan H, Yang Y, et al. The medicinal uses of the genus Bletilla in traditional Chinese medicine: A phytochemical and pharmacological review. J Ethnopharmacol. 2021;280:114263.
9. He X, Wang X, Fang J, Zhao Z, Huang L, Guo H, et al. Bletilla striata: Medicinal uses, phytochemistry and pharmacological activities. J Ethnopharmacol. 2017;195:20–38.
10. Yue L, Wang W, Wang Y, Du T, Shen W, Tang H, et al. Bletilla striata polysaccharide inhibits angiotensin II-induced ROS and inflammation via NOX4 and TLR2 pathways. Int J Biol Macromol. 2016;89:376–88.
11. Sonnenborn U. Escherichia coli strain Nissle 1917-from bench to bedside and back: history of a special Escherichia coli strain with probiotic properties. FEMS Microbiol Lett. 2016;363:19.
12. Kandasamy S, Vlasova AN, Fischer DD, Chattha KS, Shao L, Kumar A, et al. Unraveling the Differences between Gram-Positive and Gram-Negative Probiotics in Modulating Protective Immunity to Enteric Infections. Front Immunol. 2017;8:334.
13. Lynch JP, Goers L, Lesser CF. Emerging strategies for engineering Escherichia coli Nissle 1917-based therapeutics. Trends Pharmacol Sci. 2022;43(9):772–86.
14. Gao C, Cheng Q, Wei J, Sun C, Lu S, Kwong CHT, et al. Bioorthogonal supramolecular cell-conjugation for targeted hitchhiking drug delivery. Mater Today. 2020;40:9–17.
15. Begley M, Gahan CGM, Hill C. The interaction between bacteria and bile. FEMS Microbiol Rev. 2005;29(4):625–51.
16. Stojanov S, Berlec A, Štrukelj B. The Influence of Probiotics on the Firmicutes/Bacteroidetes Ratio in the Treatment of Obesity and Inflammatory Bowel disease. Microorganisms. 2020;8(11).

17. Zhu M, Wang S, Yue N, Zhao H, Zhang Y, Tian C et al. One stone three birds: Andrographis paniculata-derived exosome-like nanoparticles mitigate dextran sulfate sodium-induced colitis. Chin Med J (Engl). 2025.
18. Lou K, Luo H, Jiang X, Feng S. Applications of emerging extracellular vesicles technologies in the treatment of inflammatory diseases. Front Immunol. 2024;15:1364401.
19. Sahu K, Satapathy T, Sahu P, Chandrakar O. Nanocarrier-induced inflammation: mechanisms, immunometabolic impacts and strategies for safer design. TransMed. 2026;1(1).
20. Liu H, Song P, Zhang H, Zhou F, Ji N, Wang M, et al. Synthetic biology-based bacterial extracellular vesicles displaying BMP-2 and CXCR4 to ameliorate osteoporosis. J Extracell Vesicles. 2024;13(4):e12429.
21. Hou W, Cao Y, Wang J, Yin F, Wang J, Guo N, et al. Single-cell nanocapsules of gut microbiota facilitate fecal microbiota transplantation. Theranostics. 2025;15(5):2069–84.
22. Hou W, Hong W, Cai S, Guo D, Yan Z, Zhu J, et al. RRM2-targeted nanocarrier enhances radiofrequency ablation efficacy in hepatocellular carcinoma through ferroptosis amplification and immune remodeling. Imeta. 2025;4(5):e70067.
23. Tang X, Huang Y, Zhu Y, Xu Y. Immune dysregulation in ulcerative colitis: pathogenic mechanisms and therapeutic strategies of traditional Chinese medicine. Front Cell Dev Biol. 2025;13:1610435.
24. Tang B, Cao Y, Li J, Gao N, Gao P, Chen X, et al. Whole microbiota transplantation restores gut homeostasis throughout the gastrointestinal tract. Imeta. 2025;4(6):e70091.
25. Shi Y, Wang H, Liu B, Sheng K, Liu L, Cao Z et al. Circulating cfDNA promoter methylation: an emerging biomarker for early detection of advanced adenoma and colorectal cancer. TransMed. 2026:100004.

Figures

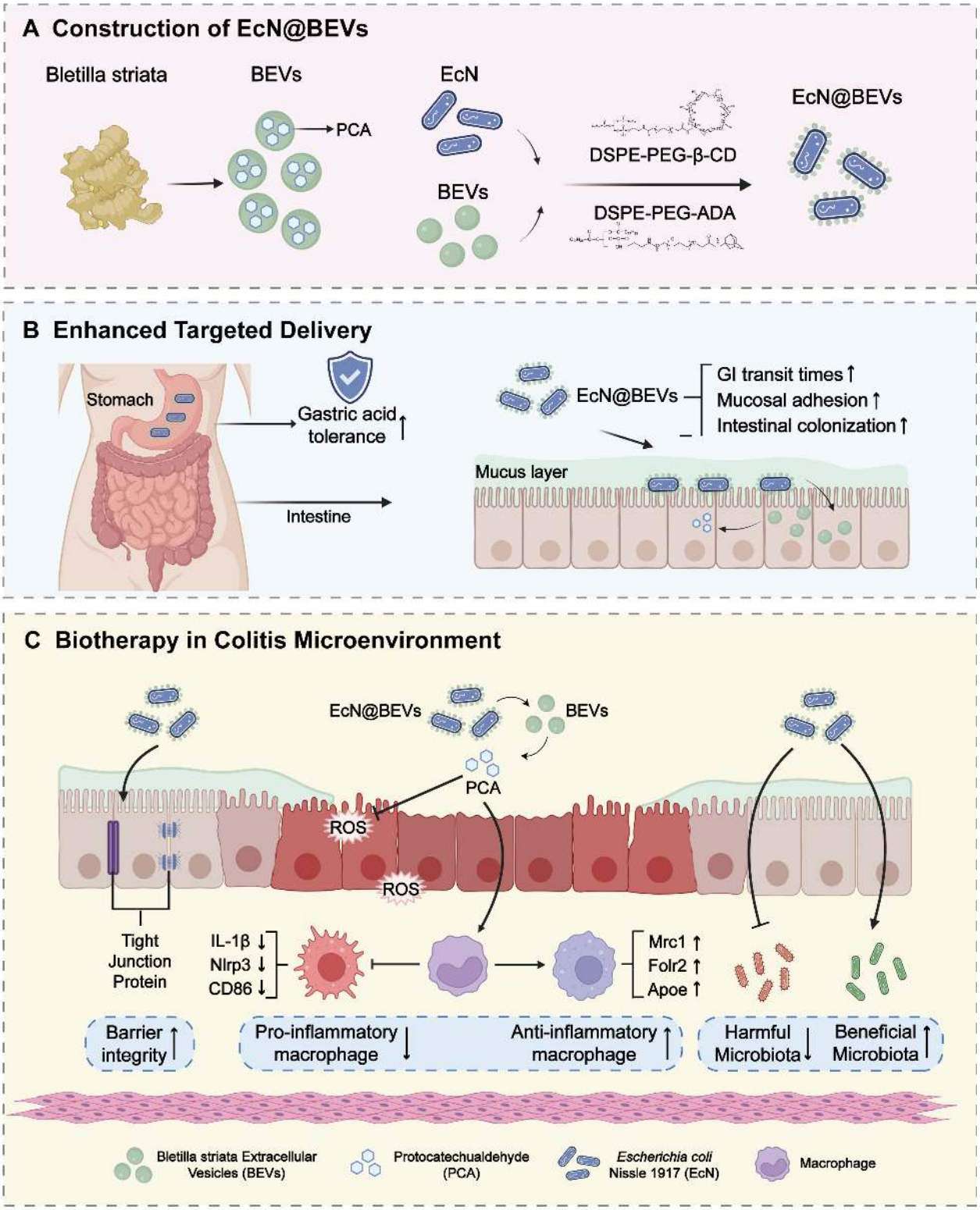

Figure 1

Schematic illustration.

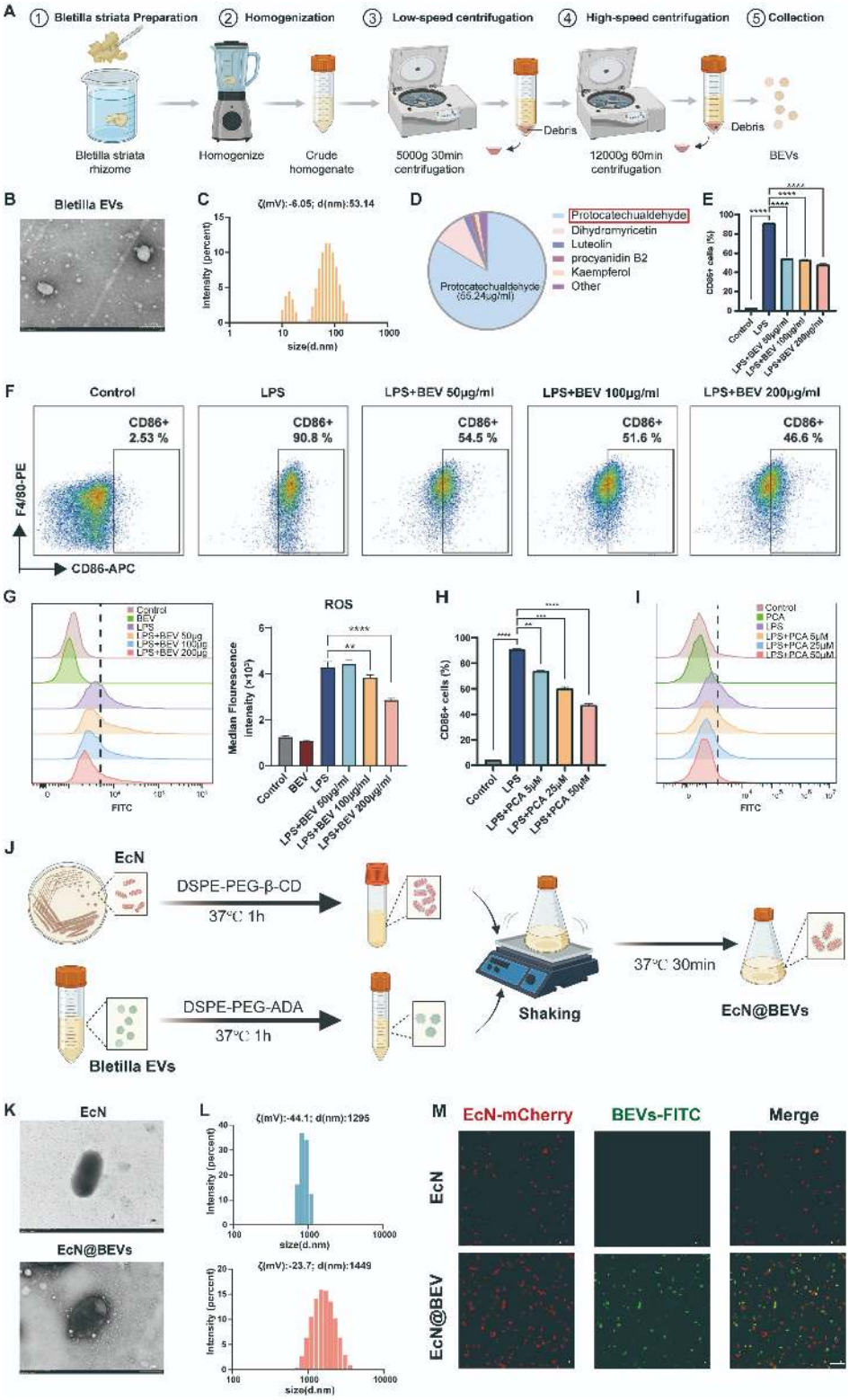

Figure 2

Preparation and characterization of BEVs and coated bacteria. (A) Schematic diagram of the process of isolating BEVs from bletilla striata rhizomes. (B) Representative TEM images of BEVs. Scale bar: 200 nm. (C) Zeta potentials and size distributions of BEVs. (D) The main components of BEVs. (E, F) Flow cytometry analyses of M1 marker CD86 of LPS-treated RAW264.7 cells stimulated by BEVs. (G) Flow cytometric histograms of RAW 264.7 macrophages treated with BEVs showing intracellular ROS (DCFH-

DA) signals. Cells were cocultured with LPS and BEVs for 24 h. (H) Flow cytometry analyses of M1 marker CD86 of LPS-treated RAW264.7 cells stimulated by protocatechualdehyde. (I) Flow cytometric histograms of RAW 264.7 macrophages treated with protocatechualdehyde showing intracellular ROS (DCFH-DA) signals. (J) The synthesis scheme of EcN@BEVs. (K) Representative TEM images of native EcN and EcN@BEVs. Scale bar: 1μm. (L) Zeta potentials and size distributions of EcN and EcN@BEVs measured by DLS. (M) Typical confocal images of EcN and EcN@BEVs. The red channel shows mCherry-expressing EcN, and the green channel indicates FITC-labeled BEVs. Scale bar:10 μm. Significance was assessed using One-way ANOVA analysis followed by Tukey's HSD multiple comparison, *$p < 0.05$, **$p < 0.01$, ***$p < 0.001$, ****$p < 0.0001$.

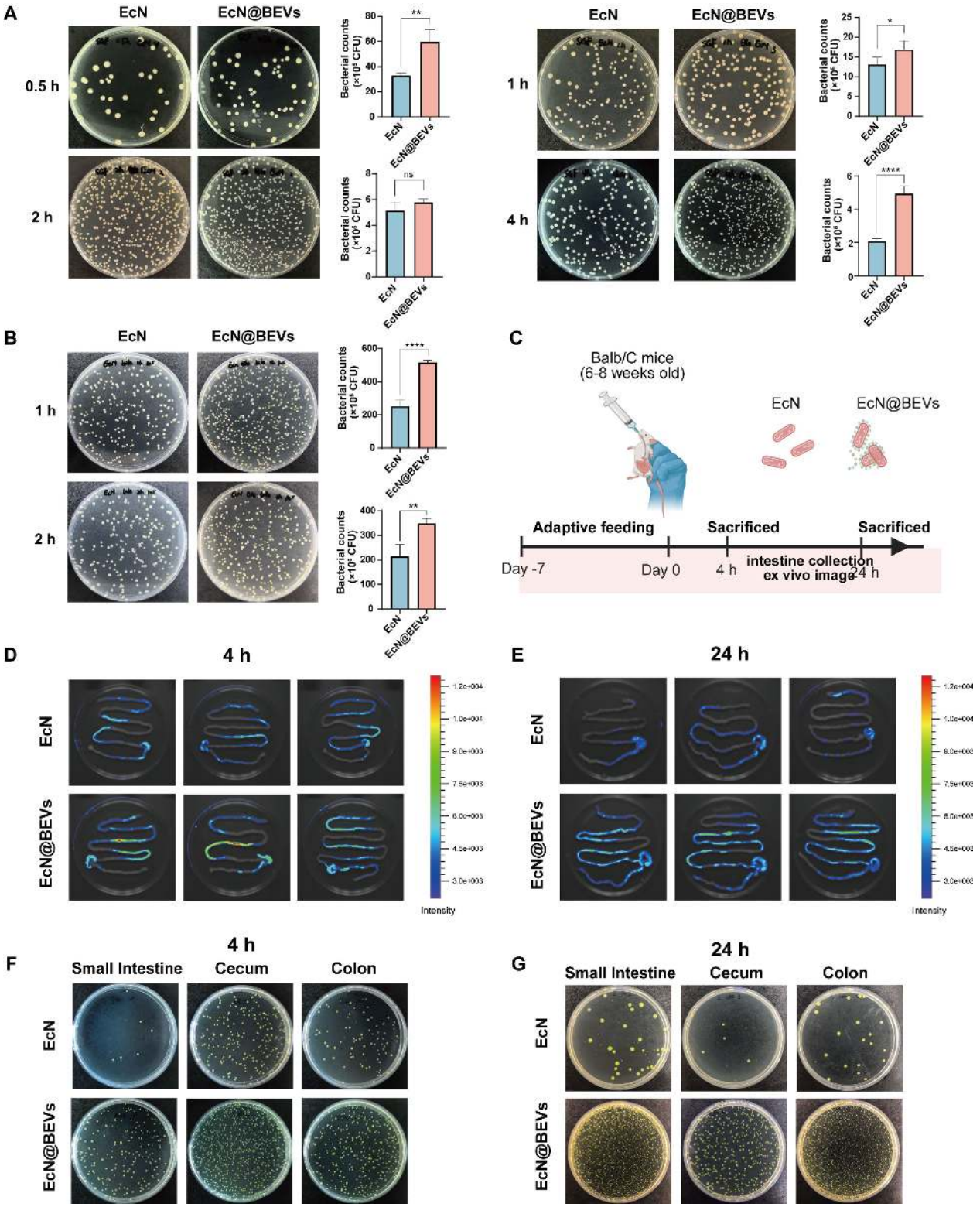

Figure 3

Enhanced Gastrointestinal Survival and Mucoadhesion of EcN@BEVs. (A) Photographs of bacterial colonies formed on agar plates of native EcN and EcN@BEVs after 0.5 h, 1 h, 2 h and 4 h incubation with SGF (pH=2) supplemented with pepsin separately. The dilution factors were 10^5 at 0.5 h, 10^4 at 1 h, and 10^3 at both 2 h and 4 h. (B) Photographs of bacterial colonies formed on agar plates of native EcN and EcN@BEVs after 1 h and 2 h incubation with bile acids (0.3 mg/ml). The dilution factors were 10^6. (C)

Schematic diagram of the experimental schedule. (D) Ex vivo survival of native EcN and EcN@BEVs retained in the GIT of healthy mice at 4 h was detected by IVIS. n = 3 per group. (E) Ex vivo survival of native EcN and EcN@BEVs retained in the GIT of healthy mice at 24 h was detected by IVIS. n = 3 per group. (F) Representative images of agar plates containing EcN collected from small intestine, cecum and colon at 4 h after oral gavage. The dilution factors were 10^4 for cecum and colon, 10^2 for small intestine. (G) Representative images of agar plates containing EcN collected from small intestine, cecum and colon at 24 h after oral gavage. The dilution factors were 10^2 for colon, 10^3 for cecum, 10^1 for small intestine. Data are presented as means ± SD (n = 3). Statistical analysis was performed using Student's t test. *$p < 0.05$, **$p < 0.01$, ***$p < 0.001$, ****$p < 0.0001$.

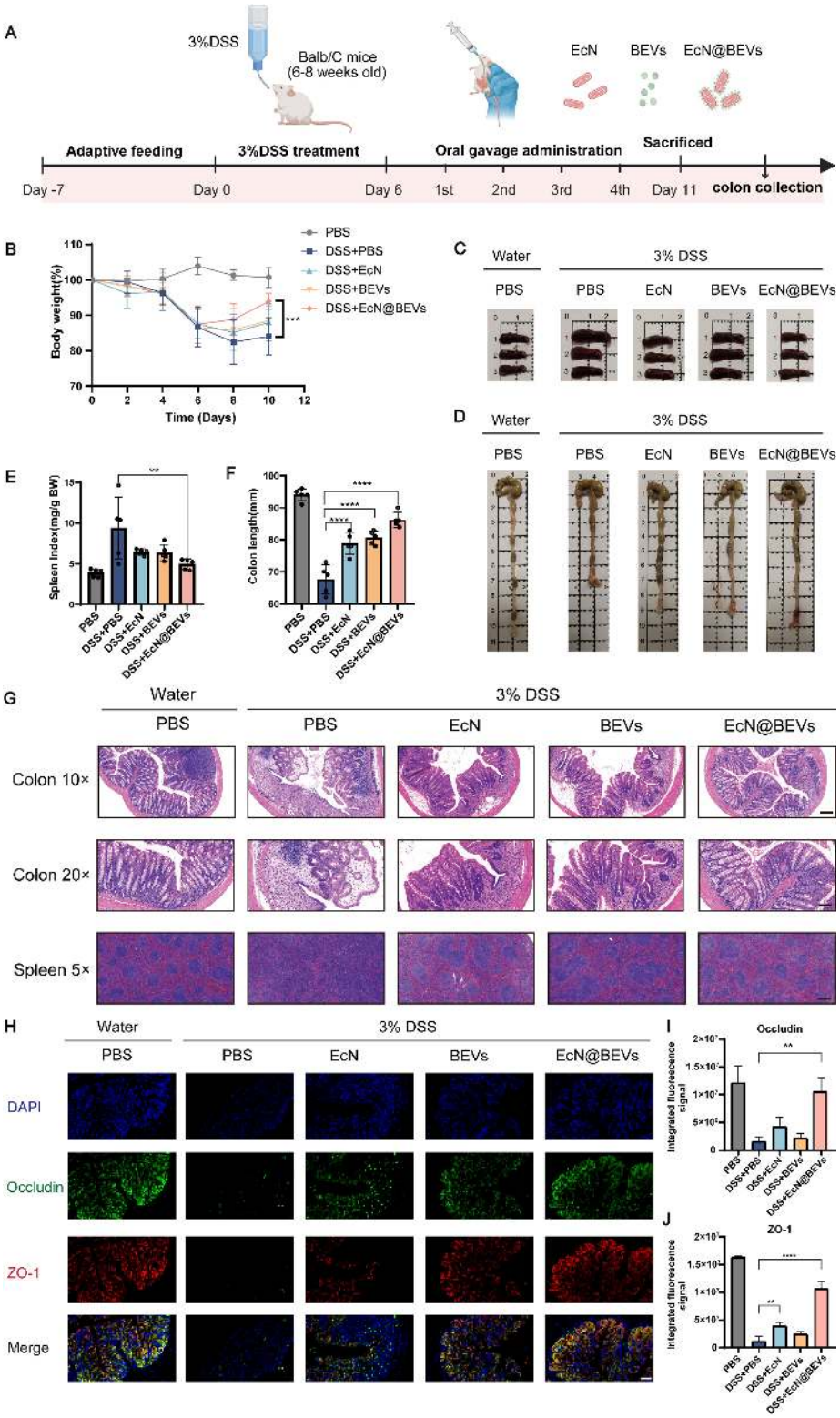

Figure 4

Therapeutic efficacy of EcN@BEVs in a mouse model of DSS-induced acute colitis. (A) Experimental scheme for establishing the DSS-induced colitis mouse model and the treatment processes. (B) Variation of body weight during the treatment for 11 days. (C, D) Images of spleen and cecum-colon tissue in each group. (E) The spleen index in different groups. (F) The length of colon tissues harvested after treatment. (G) Typical images of H&E staining of the colon and the spleen after treatment. Scale

bar: 400 μm for 5×, 200 μm for 10×, 100 μm for 20×. (H) Representative immunofluorescence images of the expression of ZO-1 and Occludin in the colon. Scale bar: 100 μm. (I, J) Semi-quantitative analysis of ZO-1 and Occludin expression levels in the colon based on immunofluorescence staining. Data are presented as means ± SD (n = 5). Significance was assessed using One-way ANOVA analysis followed by Tukey's HSD multiple comparison, *p < 0.05, **p< 0.01, ***p < 0.001, ****p < 0.0001.

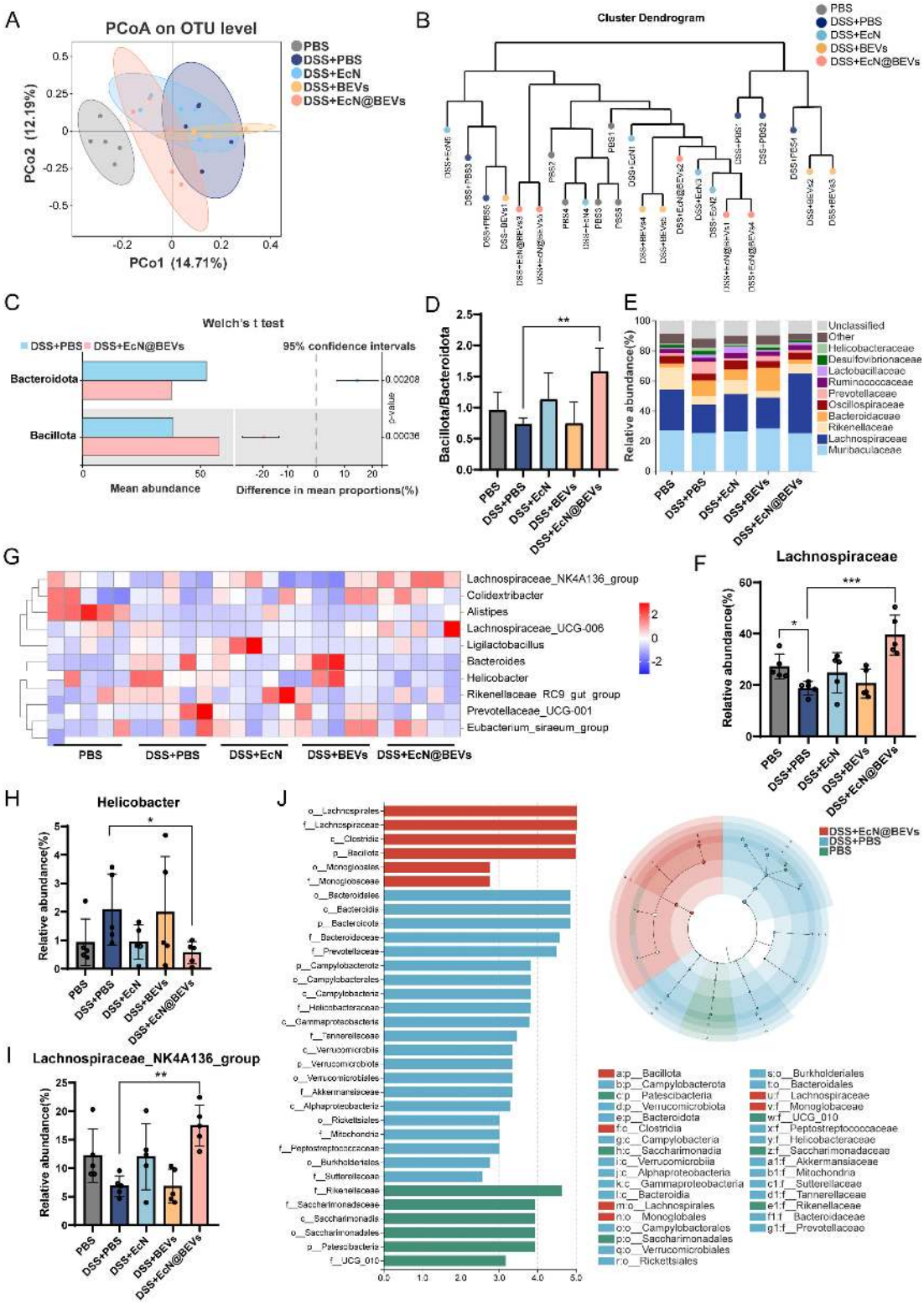

Figure 5

Regulation of the gut microbiota by EcN@BEVs in colitic mice. (A) The PCoA plot showed the β diversity of the gut microbiota in different groups. (B) Hierarchical clustering of gut microbial communities for different groups based on the UPGMA. (C) Column diagram of the mean abundance of gut microbiome at the phylum level. (D) Column diagram of the Bacillota/Bacteroidota ratio across different groups. (E) Column diagram of the relative abundance of gut microbiome at the family level. (F) Relative abundance of Lachnospiraceae. (G) Heatmap of the relative abundance of of the top 10 microbes at the genus level. (H, I) Relative abundance of Helicobacter (H), and Lachnospiraceae_NK4A136_group (I). (J) The LEfSe analysis identified the characteristic bacteria in different groups. Data are presented as means ± SD (n = 5). Statistical analysis was performed using Welch's t test and One-way ANOVA analysis followed by Tukey's HSD multiple comparison. *p< 0.05, **p < 0.01, ***p<0.001.

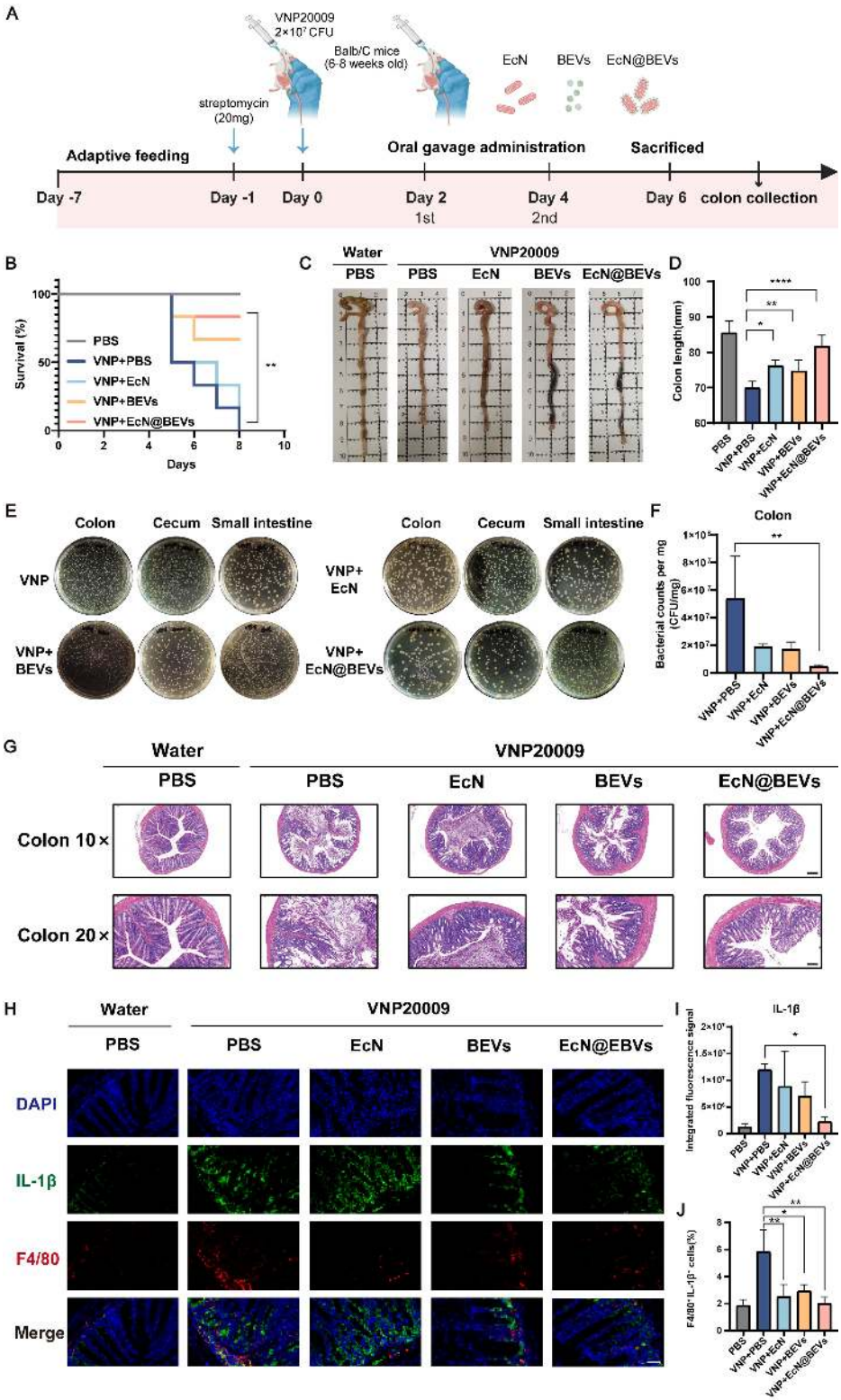

Figure 6

Therapeutic Efficacy of EcN@BEVs in Salmonella-Induced Mouse Colitis Model. (A) Experimental scheme for establishing the Salmonella-induced colitis mouse model and the treatment processes. (B) Kaplan-Meier survival curves of mice in different treatment groups. (n = 6). (C) Images of the cecum-colon tissue in each group. (D) The length of colon tissues harvested after treatment. (E, F) Bacterial smears and quantitative analysis of the small intestine, cecum, and colon across in each group (green:

EcN-GFP). (G) Typical images of hematoxylin and eosin (H&E) staining of the colon after treatment. Scale bar: 200 μm for 10×, 100 μm for 20×. (H) Representative immunofluorescence images of the expression of IL-1β and F4/80 in the colon. Scale bar: 40 μm. (I) Semi-quantitative analysis of IL-1β expression levels in the colon based on immunofluorescence staining. (J) The proportion of F4/80^{+} IL-1β^{+} cells in the colonic mucosa. Data are presented as means ± SD (n = 4). Significance was assessed using One-way ANOVA analysis followed by Tukey's HSD multiple comparison, *p < 0.05, **p< 0.01, ***p < 0.001, ****p < 0.0001.

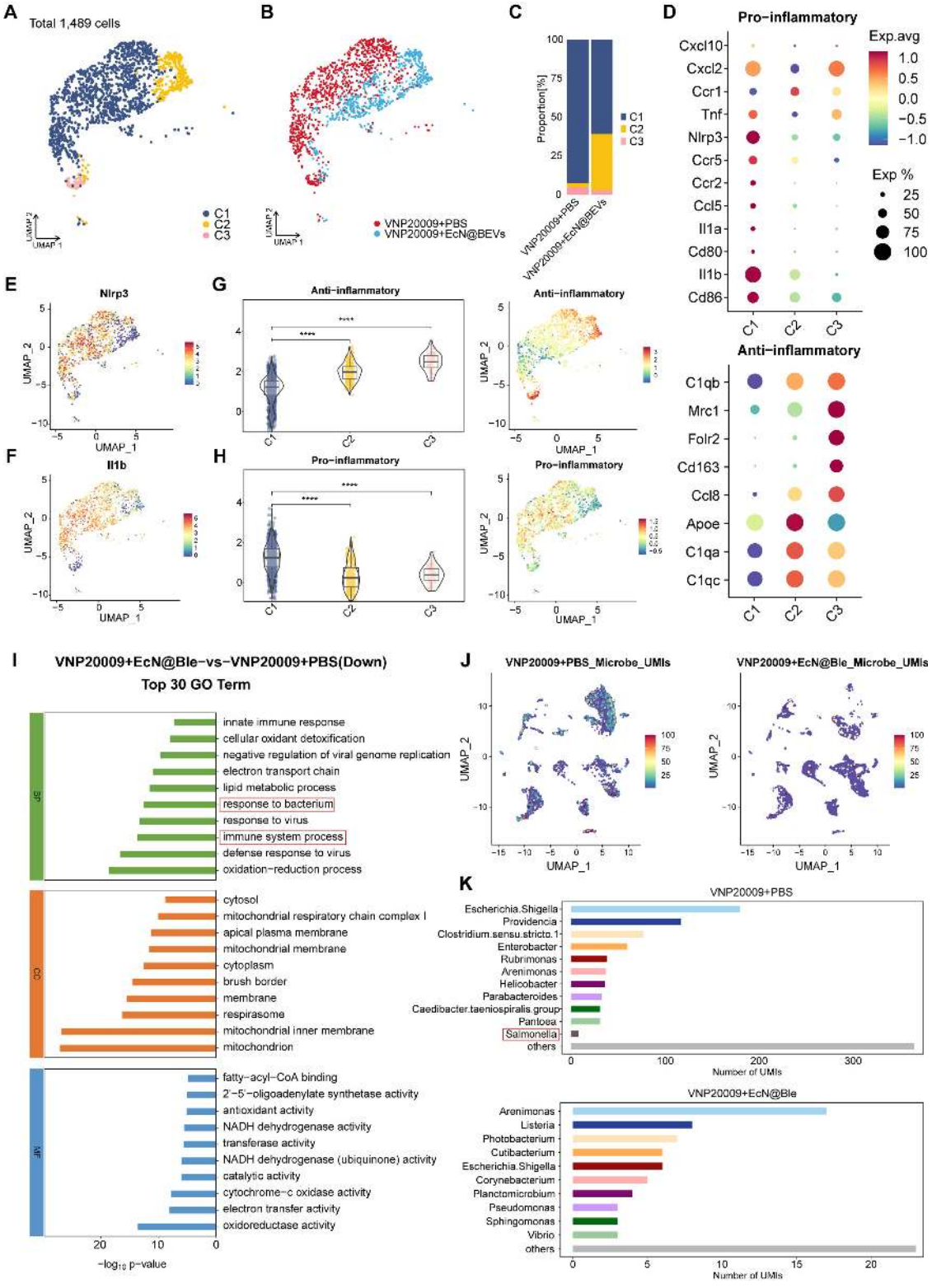

Figure 7

EcN@BEVs attenuates colitis through the regulation of macrophages. (A) UMAP plot showing cell compositions of indicated macrophage subpopulations. (B)UMAP plot showing macrophage populations across two samples. (C) Column plots of different macrophage subpopulations in two samples. (D) pro-inflammatory and anti-inflammatory genes bubble maps of indicated macrophage subpopulations. (E) Scoring based on anti-inflammatory gene modules. (F) Scoring based on pro-inflammatory gene modules. (G, H) UMAP plot showing the expression of Nlrp3 and Il1b. (I) GO pathway enrichment analysis of epithelial cells in two samples. (J) UMAP plot showing intracellular microbe-associated UMIs. (K) Bar plot of microbial UMI counts between two samples.

Supplementary Files

This is a list of supplementary files associated with this preprint. Click to download.

- supplementalmaterials.pdf